JOURNAL OF MATERIALS SCIENCE **34** (1999) 2291–2301

The effect of spray forming on the microstructure and properties of a high chromium white cast iron

D. N. HANLON*, W. M. RAINFORTH, C. M. SELLARS
The Department of Engineering Materials, The University of Sheffield, Mappin St. Sheffield S1 3JD, UK
E-mail: D.N.Hanlon@stm.tudelft.nl

The effect of spray forming on the structure and properties of a 17% Cr, 2.5% C white cast iron is described and compared with conventionally cast material of the same composition. Spray forming resulted in a substantial reduction in microstructural scale (eutectic $(Cr,Fe)_7C_3$ fields of up to 500 μm in conventionally cast material were replaced by discrete carbides of typically 2–8 μm diameter in the spray cast deposit). Carbide size varied as a function of position in the spray deposit, being approximately twice the size at mid section compared with either surface or interface with the collector. Carbide size was not altered by the gas to metal ratio used to atomise the spray. Spray forming increased transverse rupture stress and work of fracture by ~50% compared with the conventionally cast material. Forging of the spray formed material was possible at ~950 °C, without inducing carbide fracture or void formation in the matrix. Quenching into iced water from 300 °C induced extensive macroscopic cracking in the conventionally cast material whereas 400 °C was required in the spray cast material to induce similar damage. The relationship between processing, microstructure and mechanical properties is discussed.

1. Introduction

High chromium content white cast irons are widely used in industry for applications that require high resistance to wear [1]. For example, white cast irons are currently the most widely adopted materials for hot rolling mill work rolls in Europe. The high wear resistance of these materials arises from a high volume fraction (approximately 20–35%) of hard chromium carbides distributed throughout a ferrous (usually hardened martensitic) matrix. However, conventional casting techniques produce structures containing coarse, interconnected, eutectic carbides, which are detrimental to properties such as impact resistance, fracture toughness and fatigue resistance. Control of the eutectic carbide structure has long been seen as a plausible strategy for improving the mechanical integrity of white cast irons [1]. However, attempts to modify the morphology and distribution of the carbide phase by control of casting parameters and alloy additions have met with only limited success [2–7], and heat treatment does not modify eutectic carbide morphology.

The conception of the spray deposition process is usually attributed to Singer [8]. Subsequently, the most significant commercial advances have been made by Osprey Metals Ltd., the holders of the basic patents (the process is patented under the name of "The Osprey Process") and their licensees [9]. The principles of this process are well-documented [10]. Molten metal is atomised and accelerated by a high velocity gas (in the case of ferrous metals this gas is usually nitrogen) and the resulting spray of metal droplets is directed onto a substrate where it solidifies and consolidates to create a high density preform. The metallurgical advantages of the process arise from the relatively rapid cooling rates achieved prior to deposition and to the high kinetic energy of the accelerated droplets which induces high nucleation rates on impact at the surface. Ideally, the droplets cool rapidly during flight and are semi-solid just prior to impact with the collector surface. After deposition, subsequent impacts break up the solidifying structure and a mushy zone is maintained at the surface in which the nucleation frequency is high. The resulting structure is macrosegregation free, consists of fine uniform equiaxed grains and contains fine uniformly distributed primary and secondary phases. In practice, control of the casting conditions is achieved by adjusting the ratio of the atomising gas to molten spray volumes. The higher the volume of atomising gas, the smaller the atomised droplets and consequently the cooler the deposition conditions.

To date spray forming has been successfully applied to production of aluminium [11] and copper alloys [12], nickel based superalloys [13], and a wide range of ferrous alloys, including stainless steels and tool steels, in a variety of product shapes [14–17]. The process has been shown to be particularly suited to the production

* *Present address:* The Netherlands Institute for Metals Research, Rotterdamseweg 137, 2628 AL Delft, The Netherlands.

of highly alloyed tool steels for which significant structural refinement cannot be achieved within the confines of conventional casting processes and for which refinement by hot working is largely prohibited. However, the application of spray forming to the manufacture of cast irons remains largely unexplored. Early work indicated that spray forming may be unsuitable for the manufacture of grey cast irons [18]. The current work examines the spray casting of a 17% Cr, 2.6% C white cast iron (hereafter referred to as 17Cr-Fe). A conventionally cast sample of the same composition was used as a comparison. Microstructure, mechanical properties, thermal shock resistance and formability were examined as a function of processing route. The work reported here forms a preliminary study with the ultimate aim to develop the Osprey process for the manufacture of full size rolling mill work rolls [14].

2. Experimental

The chemical compositions of the high Cr white cast irons investigated are listed in Table I. Conventionally cast material was supplied by The British Rollmakers Corporation Ltd. in the form of small section (100 mm diameter) sand mould castings. Spray formed billets were supplied by Osprey Metals Ltd. All spray formed samples were produced on an experimental scale (80 mm diameter billets) by deposition onto a rotating cold mild steel tubular collector. A range of gas (nitrogen) to metal ratios was used to yield a wide range of deposition conditions at the point of impact on the collector surface, as listed in Table II. Melts for spray forming were obtained from the same feedstock material as the conventionally cast material. Table I indicates that spray forming did not alter the composition appreciably, except for small changes in C and Si levels.

The microstructures of spray cast and conventionally cast materials were characterised by optical, scanning electron microscopy (SEM) (JEOL 6400) and image analysis. The chemical composition of the carbides was determined using Energy Dispersive Spectroscopy (EDS) in the SEM. The phases present in the as-cast structures were identified by X-ray diffractometry (XRD) using a philips 1710 diffractometer. The volume of austenite present in all materials was estimated from XRD traces according to the procedure outlined by Durnin and Ridal [19]. In order to avoid contributions to integrated intensities from carbide reflections, only those iron peaks occuring at angles remote from those of the carbides (i.e. (200)α and (220)α (220)γ, and (311)γ) were included. Solid specimens mounted in a rotating specimen holder were used for this purpose in an attempt to negate the effects of preferred crystallite orientation. However, whilst the fine grained spray cast materials exhibited no preffered orientation, the coarser, highly directional dendritic structure of the conventionally cast materials was found to display a strong prefered orientation. Consequently, the errors encountered (reported as the range of austenite fractions calculated from each trace) was much greater for the conventional material. The volume fractions of eutectic carbides were determined using a Swift automatic point counting device in the optical microscope. Carbide sizes were evaluated from digitally captured images using PC based image analysis software. Each value reported is the average of a minimum of 300 measurements. A form factor, describing the shape of the carbides was also calcuated according to the expression:

$$S_f = \frac{4\pi A}{P^2}$$

Here; $A =$ carbide area and $P =$ carbide perimeter. According to this analysis S_f for a perfect circle is 1.0 whilst for a line it is 0. The shape factors for an equilateral triangle, a square and a pentagon are approximately 0.61, 0.79 and 0.86 respectively.

Resistance to thermal shock was assessed using a technique similar to that outlined by Kihara [20]. This involved rapidly induction heating a disc specimen (at approximately 225 °C min^{-1}) to 200 °C, holding at temperature for 5 minutes and subsequently quenching into iced water at 5–8 °C. After quenching, each specimen was carefully inspected for cracks. In the absence of visible cracks the specimen was re-heated in the same manner to 300 °C and quenched once more. The process was repeated at temperatures increasing each time by an interval of 100 °C until cracks were positively identified. Again, all specimens were tested in the heat-treated condition (Fig. 1).

TABLE I Chemical analyses of spray-cast and conventionally cast 17Cr cast iron

	Composition (wt %)								
Material	C	Si	S	P	Mn	Ni	Cr	Mo	Cu
Conventional	2.57	0.95	0.04	0.05	0.69	0.76	17.1	1.55	0.06
Spray cast	2.72	0.87	0.03	0.03	0.67	0.76	17.0	1.44	0.06

TABLE II A comparison of carbide sizes observed in all high chrome iron materials (the values reported for the spray cast materials are those recorded at the half radius location)

Material	Gas/Metal ratio	Area (μm^2)	Perimeter (μm)	Shape factor
Conventionally cast	NA	1618.6	441.9	0.45
Spray cast	1.69 (Cold)	6.1	12.9	0.61
Spray cast	1.29 (Medium)	6.5	16.2	0.50
Spray cast	1.07 (Hot)	7.5	17.9	0.49
Spray cast	0.97 (Very hot)	6.4	14.7	0.51

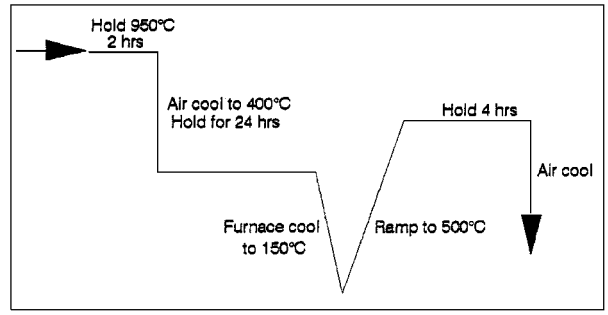

Figure 1 The heat treatment schedule applied to both conventionally cast and spray cast materials.

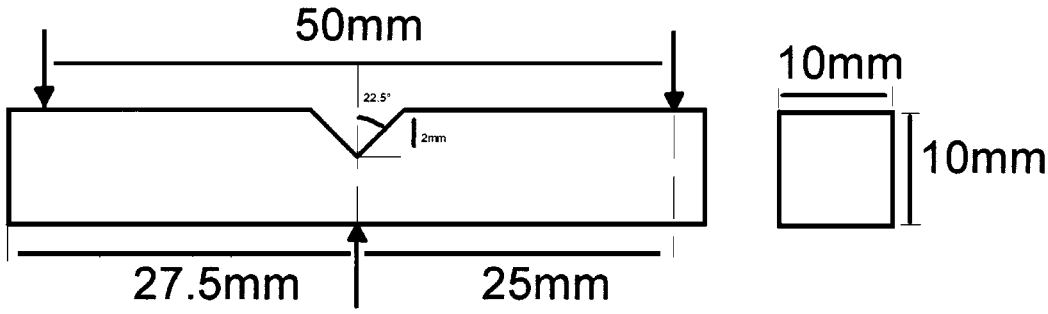

Figure 2 Diagram showing the dimensions of the specimens used for three point bend testing and the location of the loading.

Bend testing was conducted on material in the as-cast and as-spray cast conditions. A three point bend testing configuration was used to evaluate work of fracture. Notched beams (Fig. 2) were tested to failure using a Hounsfield 10 kN screw driven testing machine. Work of fracture was determined from the load deflection curves and minor differences in the geometry of the specimens was accounted for by dividing by the measured cross sectional area in each case. The final value is thus expressed as $J\,m^{-2}$. Each value reported is the average of two tests.

The hot formability of spray cast and conventionally cast materials was assessed using a hot upset forging test on ring specimens. The details of this test are reported more thoroughly elsewhere [21]. The ring specimens tested were each 50 mm in height, 54 mm in outer diameter and contained a central bore of 20 mm internal diameter. All forging trials were conducted on materials in the as-cast or as-spray cast conditions without lubrication or prior heating of the test platens. In all cases, specimens were heated to approximately 1100 °C and subsequently transferred to a 50 tonne vertical hydraulic press where they were upset forged. Forging was continued until no further reduction could be achieved. Due to heat losses on transferral from the furnace to the press, the temperature at the onset of forging was approximately 950 °C in all cases. Temperature (measured by means of an embedded k-type thermocouple), load and ram displacement were logged continuously throughout each test.

3. Results

The variations in spraying conditions (listed in Table II) did not influence the scale of the spray cast microstructure in a measurable way. Low magnification observation of the spray cast billets indicated a porous and inhomogeneous surface structure which extended to a depth of 2–3 mm, Fig. 3. Evidence that the spray contained a high fraction of solid when it impinged on the collector surface was present in this region, (for example, round prior atomised particles are visible in Fig. 3). However, below this thin layer the structure was macroscopically homogeneous and no coarse porosity was present. A few isolated pores were visible within the spray deposit, typically of a size 20–40 μm.

In the as-cast state, both processing methods produced a ferritic/austentic matrix with $(Cr,Fe)_7C_3$ (hereafter M_7C_3) carbides as would be expected at equilibrium [22]. The fraction of austenite present in the as-cast structure was comparable for both spray cast and conventionally cast materials (Table III). Subsequent to the heat treatment schedule outlined in Fig. 1, the austenite contents in both the spray cast and conventionally cast materials were significantly reduced (Table III).

Fig. 4 gives a comparison of the bulk microstructures of conventionally cast and spray cast 17Cr-Fe following

TABLE III The fraction of retained austenite in as-cast and heat treated 17Cr Fe as determined from XRD traces

Condition	Fraction retained austenite
Spray cast—very hot	0.52 (±0.05)
Conventionally cast	0.43 (±0.08)
Spray cast—heat treated	0.09 (±0.03)
Conventionally cast—heat treated	0.11 (±0.08)

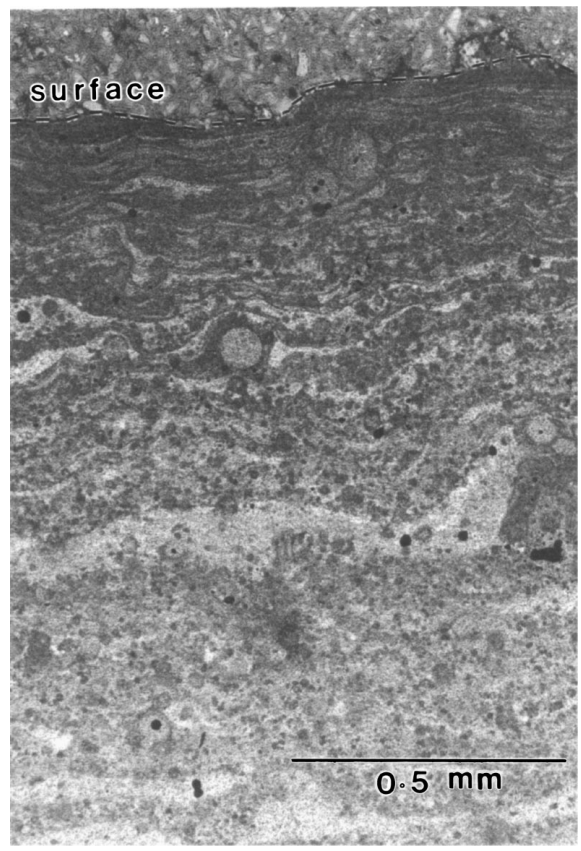

Figure 3 Low magnification optical micrograph showing the surface region of a section of a spray cast billet (etched in 2% nital).

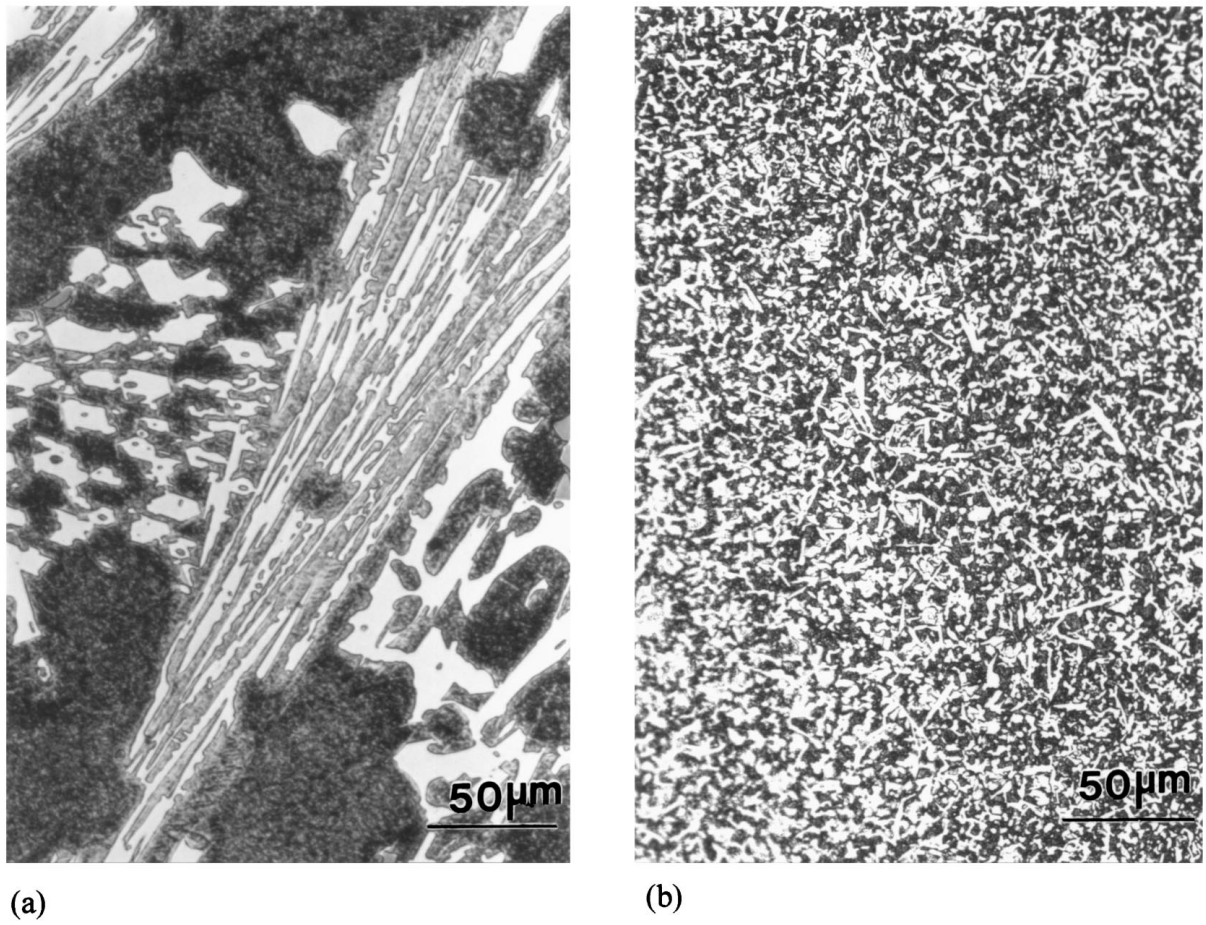

Figure 4 Optical micrographs comparing the scale of the structures observed in spray cast and conventionally processed 17Cr-Fe: (a) Conventionally cast and (b) spray cast.

a 2 h isothermal hold at 700 °C. This heat treatment decomposed much of the austenite retained in the as-cast state, allowing clearer differentiation of the carbide distribution. However, the heat treatment did not have a measurable effect on carbide size or morphology. Spray casting resulted in a dramatic refinement of microstructural scale. The carbides in the conventionally cast material were present as coarse, networked eutectic phase fields (eutectic fields of up to 500 μm in length were observed) while carbides in the spray formed material were discrete (typically 2–8 μm in diameter) and more uniformaly distributed. The average area, perimeter and shape factors measured for each of the spray cast and conventionally cast materials are compared in Table II.

A variation in the scale of the cast structure with depth below the billet surface was found, with the coarsest structure occurring at the half radius location (Fig. 5). Fig. 6 gives the area of the individual carbide particles and Fig. 7 the perimeter of the carbide, both as a function of position within the deposit expressed as the radial fraction (r/R), from which it can be seen that the coarsest structure occurred in mid-section. Interestingly, the decrease in carbide size at the surface and basal regions of the preform was associated with a measurable change in the carbide morphology. Fig. 8 shows that the shape factor varied from approximately 0.65 and 0.7, at the substrate and surface respectively, to approximately 0.5 at the mid radial location indicating that the finer carbides are more globular. The carbide size and shape did not vary appreciably as a function of the gas to metal ratio used to atomise the spray (Figs 6–8).

TABLE IV Volume fraction of carbides in spray cast and conventionally cast materials as determined by point counting

Carbide volume fraction	
Conventional	Spray-cast
0.28 (±0.06)	0.31 (±0.05)

TABLE V Quantitative EDS results showing the analysis of carbides found in the spray-cast and conventionally processed 17Cr-Fe

		As spray cast	Conventional
Phase	Element	Atom %	Atom %
Matrix	Fe	89	89
	Cr	10	10
	Mo	1	1
	W	0	0
Carbide	Fe	51	46
	Cr	47	52
	Mo	2	2
	W	0	0

The volume fraction of carbides present in the spray cast and conventionally cast materials was essentially the same (Table IV). Quantitative EDS of the carbides indicated that their composition was approximately the same in each of the materials (Table V).

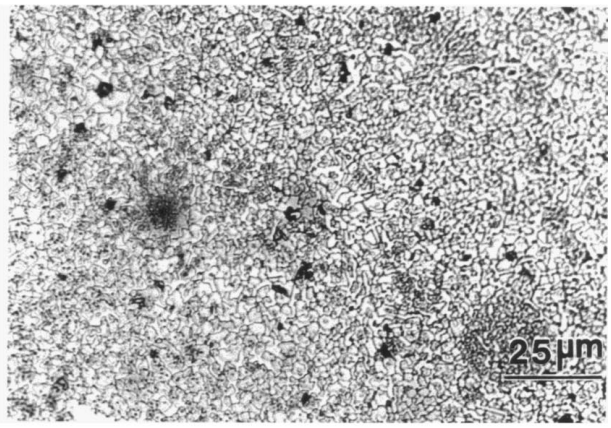

(a) Near surface (r/R≈1)

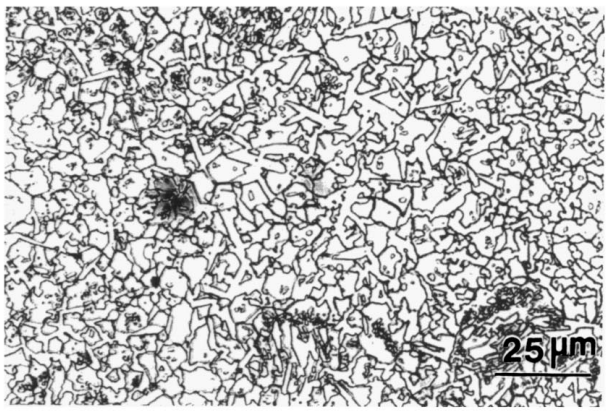

(b) Near centre (r/R≈0.5)

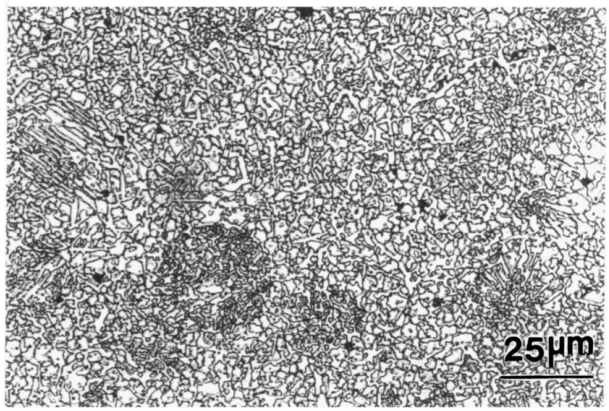

(c) Near substrate (r/R≈0)

Figure 5 Micrographs comparing the scale of the structure observed through the radius of the spray cast preforms.

Table VI gives the bend test results (each value is the average of two tests), in which the energy to fracture (a measure of toughness) has been evaluated from the area under the load/deflection curve (Fig. 9). It is apparent from these results that the bend toughness of the spray cast material is consistently greater than that of the conventionally cast material (the values recorded represent a 50% increase).

TABLE VI Bend test data for conventional and spray cast specimens

Material	Energy to fracture (J)	Specimen cross sectional area (mm^2)	Energy to fracture per unit area (kJ/m^2)
Conventionally cast 17Cr-Fe	0.85	99.6	8.5
Spray cast 17Cr-Fe	1.30	99.1	13.1

TABLE VII Summary of thermal shock observations

	Observations		
Material	200 °C/Quench	300 °C/Quench	400 °C/Quench
Conventionally cast 17Cr-Fe	No visible cracks	Extensive cracking	—
Spray cast 17Cr-Fe	No visible cracks	No visible cracks	Extensive cracking

TABLE VIII Summary of forging trials

Specimen	Temperature at onset of deformation (°C)	Appearance after forging	Forging reduction (%)
Conventionally cast	969	Heavily cracked	36
Conventionally cast	950	Cracked	38
Spray-cast	919	No cracking central bore fully closed	50
Spray-cast	Temperature readout failed	No cracking central bore fully closed	47

The observations of the thermal shock experiments are given in Table VII. The first visible cracks in the conventional material appear after quenching from 300 °C while those in the spray cast material appear after quenching from 400 °C. This indicates that the thermal shock resistance of the spray cast material is higher than that of the conventional 17Cr-Fe material.

The results of forging trials are summarised in Table VIII. These show that the spray cast material exhibits superior formability compared with its conventionally cast counterpart. The forging reduction achieved for the spray cast materials was 47–50% while that for the conventionally cast material was 36–38%. On completion of forging, the conventionally cast specimens were found to be heavily cracked (Fig. 10). In contrast, no evidence of macroscopic cracking was observed in spray cast specimens after forging to the greater reduction of 49%. Therefore, the forging reduction data apparently gave a conservative measure of the formability of the spray cast material.

The microstructures of the two materials after forging are compared in Fig. 11. The large eutectic carbides in the conventionally cast material were extensively fractured (Fig. 11a). In some locations the collapse of large fields of eutectic carbides had resulted in clusters of fractured carbide separated by thin layers of matrix material. In contrast, no carbide fracture was positively observed in the spray cast material (Fig. 11b), and the

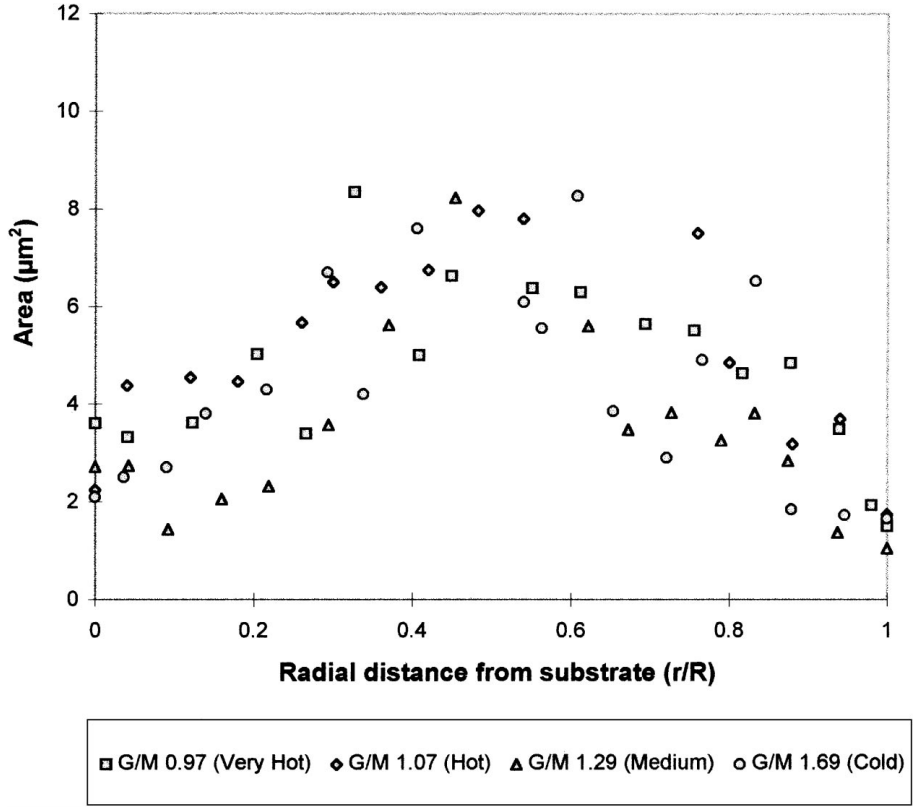

Figure 6 Area of M_7C_3 as a function of radial location in the spray deposit for three different gas/metal ratios.

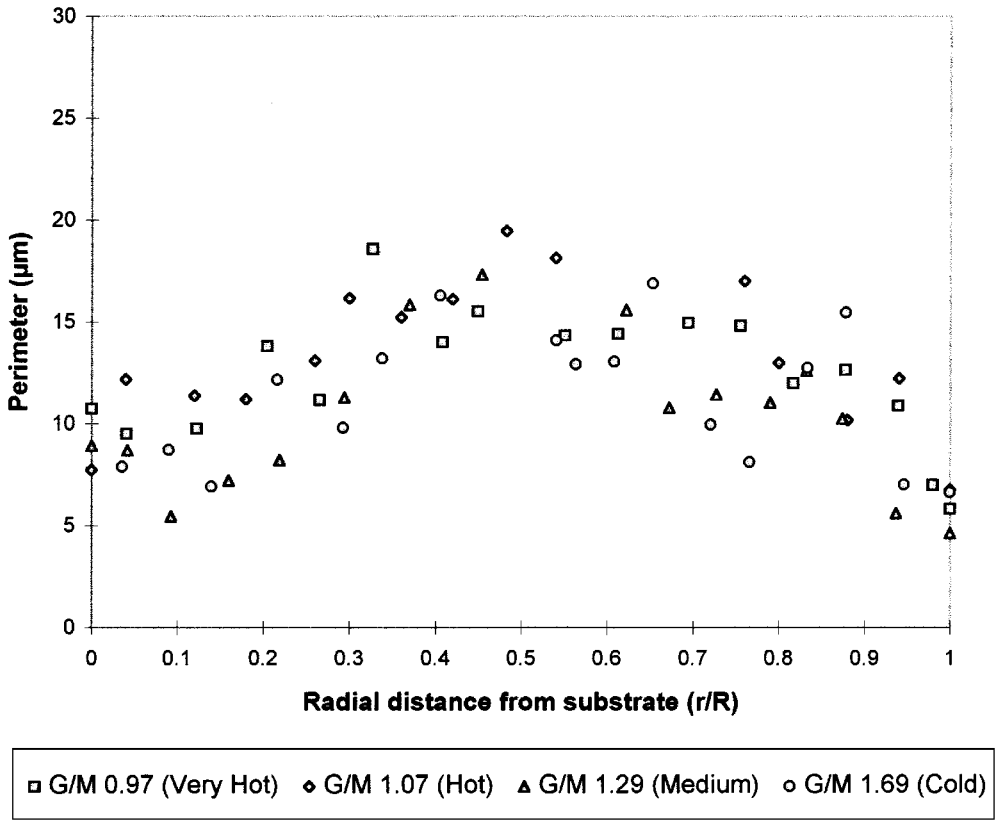

Figure 7 Perimeter of M_7C_3 as a function of radial location in the spray deposit for three different gas/metal ratios.

uniform distribution of the carbide present in the as-cast spray formed state was maintained after forging.

The load displacement curves from the forging experiments were significantly different for spray cast and conventionally cast materials, Fig. 12. In the case of the conventionally cast material, load increased rapidly to a maximum value (the load capacity of the press used) and remained at this maximum until the capacity of the press was insufficient to induce further displacement. For the spray cast material, yielding occurred at

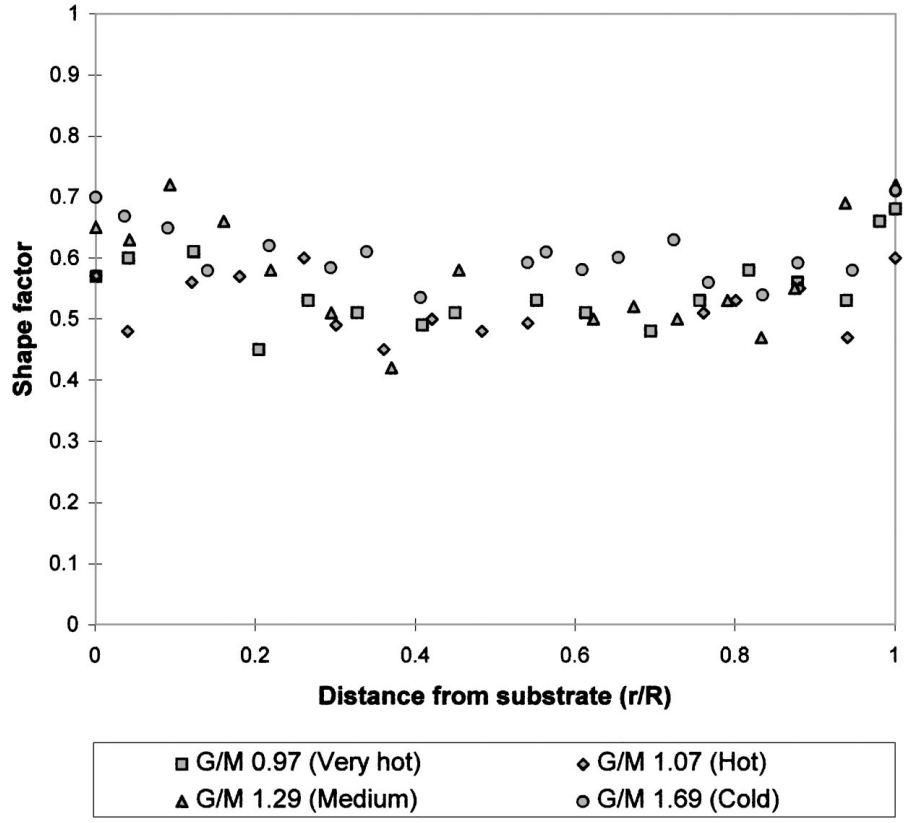

Figure 8 Shape factor of M_7C_3 as a function of radial location in the spray deposit for three different gas/metal ratios.

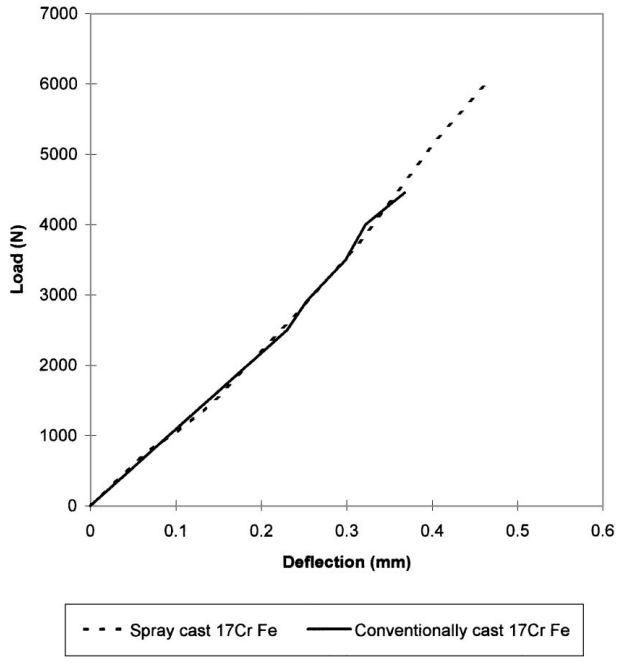

Figure 9 Load deflection curves for notched 3-point bend specimens.

a lower applied load than for the conventional material. The flow stress increased continuously up to the machine's capacity with increasing strain (as a result of the falling work piece temperature, Fig. 13).

4. Discussion

4.1. Microstructure

A high density (>99% theoretical) preform of high alloy white cast iron has been produced by spray forming. Only in the outer 2–3 mm of the billet radius and in the basal region close to the substrate (in total approximately 10% of the deposit thickness) was there evidence of significant porosity or microstructural inhomogeneity. These findings compare favourably with those of Ebalard and Cohen [18] whose attempts to spray form a grey cast iron were largely unsuccessful. These authors reported a layered structure, similar to that observed in the near surface region in the work reported here, which persisted throughout the

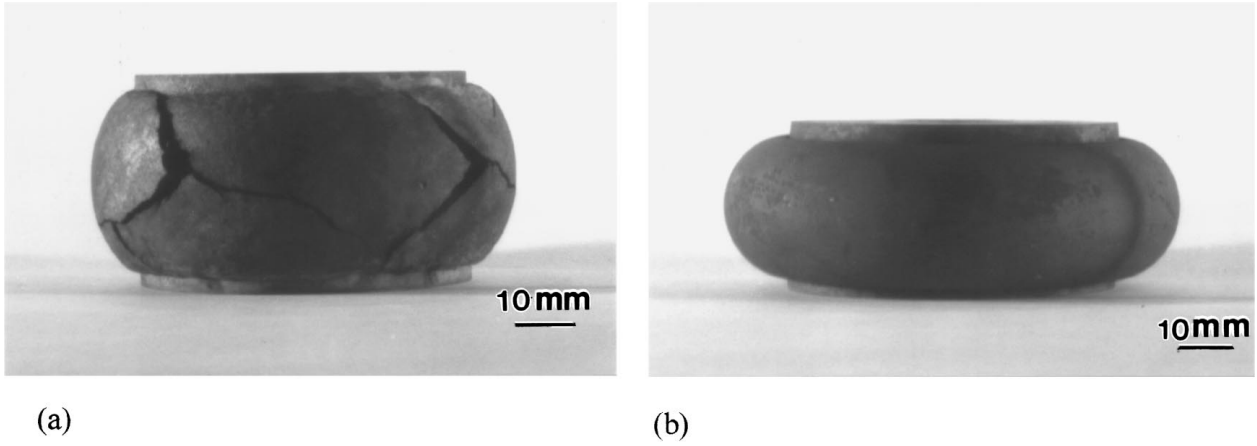

Figure 10 Photographs of forged specimens after maximum reduction: (a) conventionally cast material and (b) spray cast material.

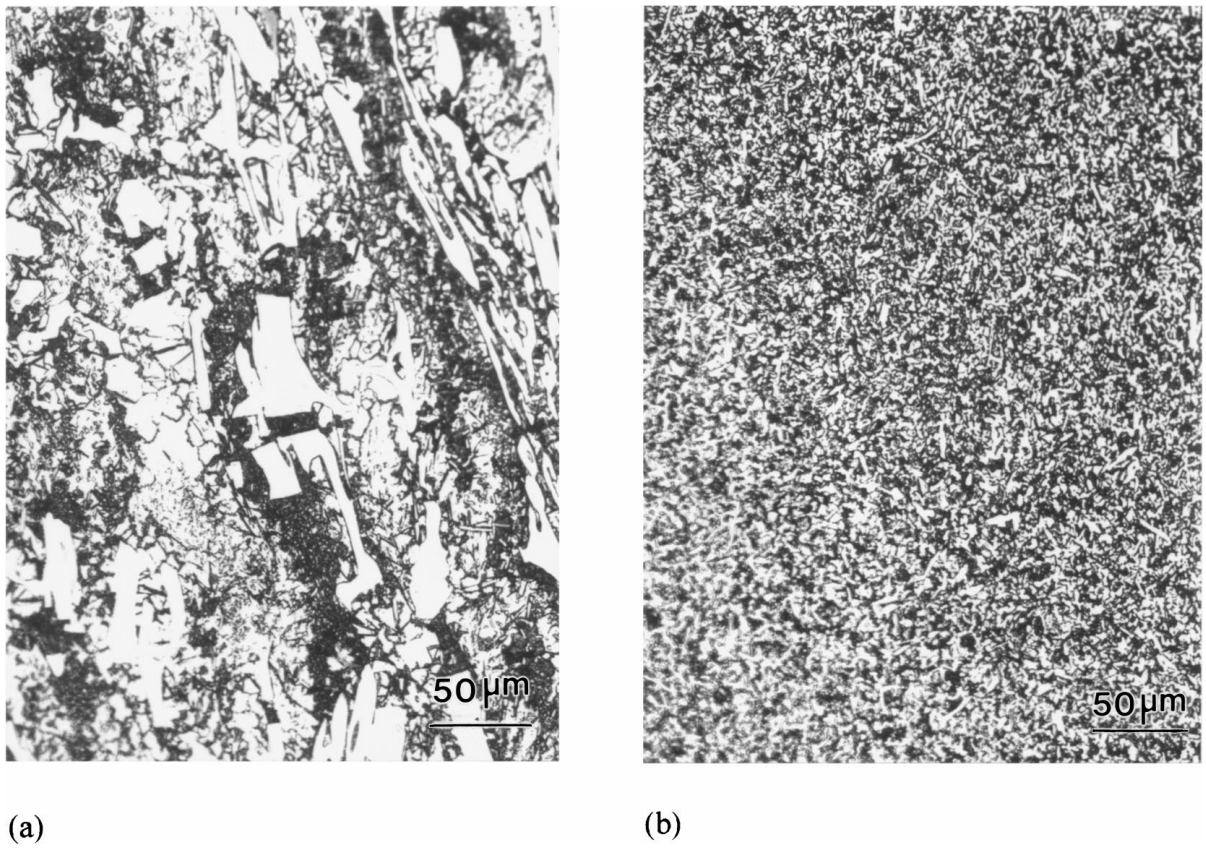

Figure 11 Optical micrographs of forged specimens: (a) conventionally cast and (b) spray cast.

entire preform cross section. The boundaries of these layers, and of prior atomised droplets, were decorated with graphite, which significantly reduced mechanical strength. Using higher rates of deposition, for which the temperature of the deposition surface of the billet was raised above the liquidus temperature, Ebalard and Cohen avoided the formation of this embrittling layered structure. However, since under these conditions the deposit surface was entirely liquid the formation of large spherical gas pores then occurred.

The poor integrity of the surface regions observed in the work reported here is thought to result from relatively rapid cooling of the deposit at the outer surface after the completion of deposition, and is common in spray cast preforms [10]. Nevertheless, such thin (2–3 mm) surface layers would be removed during subsequent processing (e.g. machining) and therefore do not represent a process problem.

The observed variation in scale of the structure across the billet radius (Figs 6–9) is associated with an increase in cooling rate in the surface and basal regions of the preform. In the basal region rapid cooling is associated with deposition onto the cold substrate and the consequent heat losses by conduction (this also inevitably results in local porosity). As the layer thickness increases the influence of the substrate diminishes and the cooling rate decreases since deposition is onto hot spray formed material. In thick section spray deposits, a steady state may be achieved which results in a constant microstructural scale until the surface is approached. At the end of deposition, rapid heat losses occur at the surface by convection or radiation resulting in

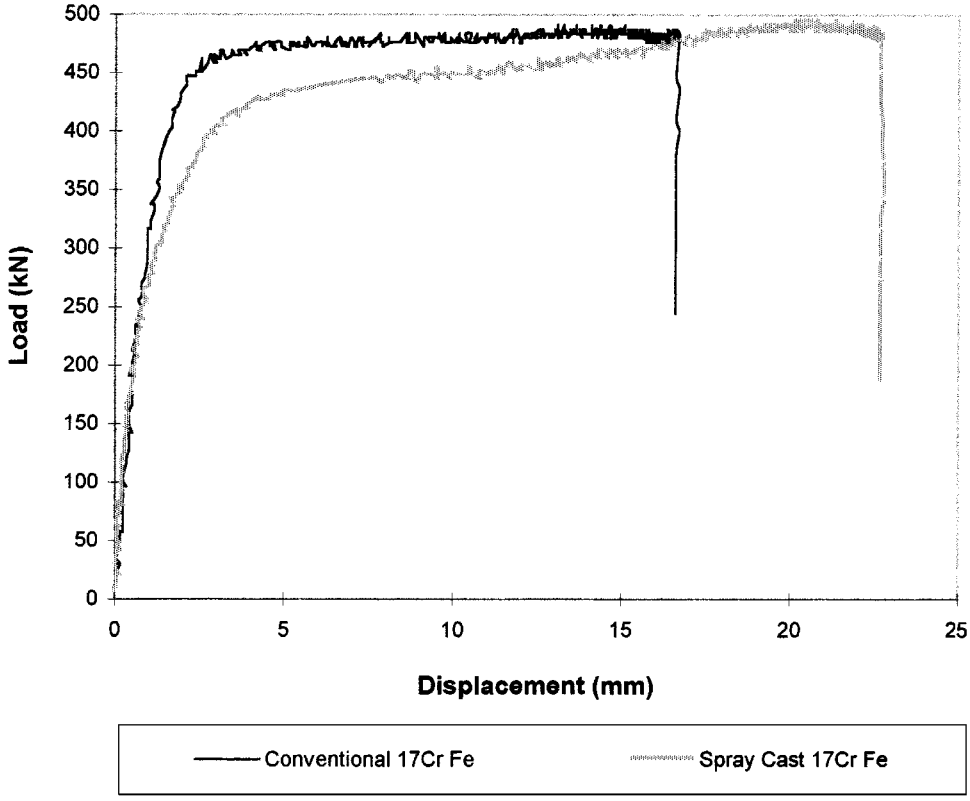

Figure 12 Load displacement curves recorded during forging of conventionally cast and spray cast materials.

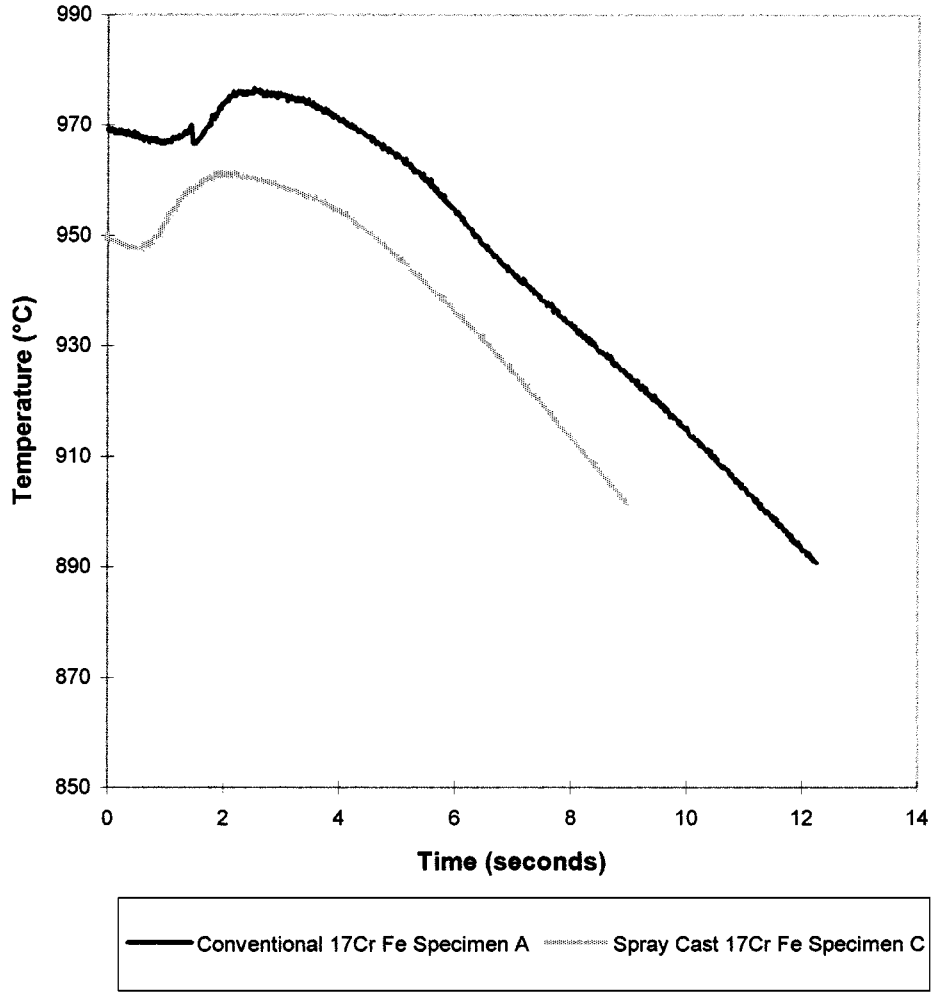

Figure 13 Forging temperature as a function of displacement for spray cast and conventionally cast materials.

a refinement of structure. The variation of microstructural scale as a function of radial position within a spray deposit has been investigated experimentally and modelled for Al-4% Cu by Grant *et al.* [10, 23]. These authors found a strong correlation between the scale of the microstructure and both predicted and measured values of surface temperature across the billet radius. In agreement with the current work, a refinement of structure was found adjacent to the substrate. Grant *et al.* also observed a reduction in microstructural scale at the free surface. However, this was over a substantially smaller distance than that observed in the present work. Grant *et al.* attributed this refinement to heat losses from the surface due to convection. One explanation for the differences in surface behaviour observed may lie in the greater efficiency of cooling at the free surface of the 17Cr-Fe compared with the Al-Cu alloy due to the additional radiative cooling expected in the former. Clearly, the extent to which this surface effect influences the spray cast microstructure will depend on the thickness of the deposit. Thicker deposits will be dominated by the steady state regime, and this has been demonstrated recently on full-size hot mill work rolls [14].

The gas to metal ratio used to atomise the liquid metal did not appreciably alter the scale of the microstructure. A high gas to metal ratio induces smaller liquid droplets, therefore more rapid cooling in-flight and consequently a greater solid fraction at the point of impact on the collector surface [10]. For example, 10 μm diameter droplets of Al-Cu (produced by a high gas/metal ratio) are cooled at 333 K s^{-1}, whereas 200 μm diameter droplets of the same alloy (produced by a low gas/metal ratio) will be cooled at 21.8 K s^{-1}. It is therefore surprising that a change in gas/metal ratio from 1.69 to 0.97 (Table II) did not induce a significant change in microstructural scale. The absence of change in microstructural scale implies that the scale of the carbide was dictated by processes within the mushy zone after impact of the semi-solid droplet, not during flight. This is also evidenced by the strong influence of post deposition cooling conditions on the scale of the microstructure, as discussed above. The fine structures associated with spray forming are partly a result of the disruption of growing nuclei by impact of subsequent droplets at the surface, which induces high nucleation rates. This therefore implies that the droplet impact conditions were similar for the range of gas/metal ratios used here. Grant [10] points out that for solid fractions prior to deposition of up to 0.4, the solid fraction proportion does not significantly alter the droplet spreading behaviour on impacting the collector surface. While the solid fraction at impact was not measured in the current work, it is probable that it was less than 0.4 since solid fractions >0.4 lead to 'cold' porosity in the final deposit (which was not the case in the bulk of the deposit).

The volume fraction of eutectic carbides in white cast irons is expected to increase with cooling rate [2]. In the present work, the carbide volume fraction was similar for both spray cast and conventionally cast materials, suggesting that the substantially higher cooling rate in the spray cast material was not important in this respect. Moreover, the spray casting did not alter the phases present, with $(Cr,Fe)_7C_3$ being the only carbide present in the as cast condition in both cases.

Not withstanding the regional variations in microstructural scale, it is apparent that spray casting led to a dramatic refinement of microstructure. The coarse, interconnected eutectic carbides typical of white irons in the conventionally cast condition were not present after spray casting. In contrast, the material contained discrete, small (typically 2–4 μm in diameter) and uniformly distributed carbides. Furthermore, the heterogeneities associated with a dendritic structure were avoided. Previous attempts to control the structure of alloy white cast irons have been reported by various authors [2–7]. Rapid cooling through the use of chills and the employment of lower superheats during casting have both been shown to increase the nucleation frequency of the carbide phase in white irons, leading to a refinement of the eutectic structure. For example, Fischer [2] found that the size, volume fraction and morphology of the eutectic carbides varied with distance from a cast iron chill plate for a Nihard white cast iron. Immediately adjacent to the chill, the carbide volume fraction was a maximum and the size a minimum. The morphology of the carbide varied from high aspect ratio "wheat-like" clusters to more discrete globular forms as the chill was approached. However, the refinement associated with the chill was limited to relatively thin sections (<50 mm) and therefore this strategy for reducing carbide size is not appropriate to the manufacture of large items. Alternative strategies have relied on the adjustment of alloy chemistry. For example, boron [3], silicon [3, 4] and antimony [7] additions have been investigated. Si additions may refine the carbide structure [3], although other work [4] indicates that Si can also have the opposite effect and reduce carbide nucleation rate. Similar controversy exists for the additions of rare-earth elements [5, 6].

It would appear that each of the above strategies has had only limited success. Furthermore whilst a degree of control over the morphology of eutectic carbides may be possible, no evidence has been presented to suggest that the formation of a dendritic microstructure has been suppressed. By its very nature interdendritic eutectic solidification will lead to inteconnected networks of carbide. The morphology of the carbides within the eutectic is thus only one of the factors which will influence mechanical integrity. In this context, spray forming offers a significantly better strategy for microstructural refinement through its effect on both carbide morphology and distribution.

4.2. Mechanical properties

It is well documented that spray forming, through its refinement of microstructure, gives rise to an enhancement of mechanical properties [11]. Furthermore, spray casting allows the production of alloy compositions which cannot be processed via conventional means [24].

The improved thermal shock resistance and greater toughness of the spray formed material compared with

its conventionally cast counterpart is directly related to the refinement and homogenisation of the microstructure, in particular the scale and distribution of the chromium carbides. Interconnected carbides in conventionally cast material provide potent crack initiation sites and an easy crack propagation path. In the spray cast material, the carbides were largely discrete, such that a higher proportion of crack propagation would be in the tougher matrix than for the conventionally cast material. Furthermore, carbides of size 2–4 μm would be less prone to fracture themselves and so are less likely to give rise to fracture initiation.

Forging the conventionally cast 17Cr-Fe led to extensive carbide fracture. This is a necessary process for carbide refinement, but inevitably leaves fractured carbides and voids. Nevertheless, Woguang *et al.* [25] have demonstrated that an improvement in toughness can result from forging a range of Mn white irons even where carbide fracture remains, although the sizes of the carbides investigated were smaller than those in the conventionally cast material examined here. The discrete carbides in the spray cast material allowed flow of the matrix around the carbides during forging, promoting a lower flow stress for this material compared with the conventionally cast 17Cr-Fe [22]. The limit of reduction for the spray cast white iron resulted from cooling of the workpiece, which increased flow stress above the capacity of the press. No carbide fracture was observed after forging indicating that higher reductions would be possible on re-heating. Thus, forging may be regarded as a realistic secondary process route for the spray cast material.

5. Conclusions

(i) Spray forming results in a substantial reduction in microstructural scale of 17Cr-2.6% C cast iron. In conventionally cast material, eutectic M_7C_3 fields of up to 500 μm were present, whereas spray forming yielded discrete, uniformly distributed, carbides of 2–8 μm.

(ii) Carbide size varied as a function of position in the spray deposit, being approximately twice the size at mid section compared with either surface or interface with the collector.

(iii) Carbide size was not changed appreciably by the gas to metal ratio used to atomise the spray.

(iv) The refinement in microstructure from spray forming resulted in an increase in transverse rupture strength and work of fracture of $\sim$50% compared with the conventionally cast material.

(v) The spray formed material could be forged without carbide fracture or void formation in the matrix.

References

1. C. P. TABRETT, I. R. SARE and M. R. GHOMASHCHI, *Int. Met. Rev.* **41** (1996) 59–82.
2. J. J. FISCHER, *Trans. AFS* **91** (1983) 47–54.
3. J. SHEN and Q. D. ZHOU, *Cast Met.* **1** (1988) 79–85.
4. G. LAIRD and G. L. F. POWELL, *Met. Trans.* **24A** (1993) 981–988.
5. G. Y. LIANG and J. Y. SU, *Cast Met.* **4** (1991) 83–88.
6. F. HAN and C. WANG, *Mater. Sci. Technol.* **1** (1989) 79–85.
7. J. LEE and R. W. SMITH, Conf. Proc. S.P. 97, edited by J. Beech and H. Jones (Sheffield, 4th–12th July, 1997) pp. 481–484.
8. A. R. E. SINGER, *Metall. Mater.* **4** (1970) 246–250.
9. R. W. EVANS, A. G. LEATHAM and R. G. BROOKS, *Powder Metall.* **28** (1985) 13–20.
10. P. S. GRANT, *Prog. Mater. Sci.* **39** (1995) 497–545.
11. M. DESANCTIS, *Mater. Sci. Eng.* **A141** (1991) 103–121.
12. R. P. SINGH, A. LAWLEY, S. FRIEDMAN and Y. V. MURTY, *ibid.* **A145** (1991) 243–255.
13. M. G. BENZ, T. F. SAWYER, W. T. CARTER, R. J. ZABALA and P. L. DUPREE, *Powder Metall.* **37** (1994) 213–218.
14. J. FORREST, R. PRICE and D. HANLON, *Int. J. Powder Metall.* **33** (1997) 21–29.
15. D. N. HANLON, W. M. RAINFORTH, C. M. SELLARS, R. PRICE, H. T. GISBORNE and J. FORREST, *J. Mater. Sci.* **33** (1998) 3233–3244.
16. M. IGHARO and J. V. WOOD, *Powder Metall.* **32** (1989) 124.
17. T. HARADA, T. ANDO, R. C. O'HANDLEY and N. J. GRANT, *Mater. Sci. Eng.* **A133** (1991) 780–784.
18. S. EBALARD and M. COHEN, *ibid.* **A133** (1991) 297–300.
19. J. DURNIN and K. A. RIDAL, *J.I.S.I* **206** (1968) 60–67.
20. J. KIHARA, Findings of the Research Committee on Rolling Rolls, *ISIJ* (1995) 17–25.
21. V. G. RIVLIN, *Int. Met. Rev.* **29** (1984) 299–327.
22. D. N. HANLON, Y. H. LI, W. M. RAINFORTH and C. M. SELLARS, *J. Mater. Sci. Lett.*, in press.
23. P. S. GRANT, P. P. MAHER and B. CANTOR, *Mater. Sci. Eng.* **A179/A180** (1994) 72–76.
24. J. A. JUAREZ-ISLAS, R. PEREZ, P. LENGSFELD and E. J. LAVERNIA, *ibid.* **A179/A180** (1994) 614–618.
25. LI WOGUANG, A. J. BAKER and P. R. BEELEY, *Cast Metals* **2** (1989) 62–70.

Received 27 October
and accepted 18 November 1998